Chapter 10

High Performance Membrane Electrode Assemblies by Optimization of Processes and Supported Catalysts

Chanho Pak, Dae Jong You, Kyoung Hwan Choi and Hyuk Chang

Additional information is available at the end of the chapter

http://dx.doi.org/10.5772/53683

1. Introduction

Recently, the mitigation of the greenhouse-gases (GHG) is the important issue to solve climate changes caused by the global warming. According to the international energy agency (IEA) report at 2010 (IEA, 2010), 65% of all GHG emissions can be attributed to energy supply and use. In addition, according to the blue scenario of IEA, all areas will need to reduce the CO_2 emission drastically until 2050, when level of CO_2 emission should be halved. In a view of energy supply and use, fossil fuels are used mainly in transport and power sectors which generate electricity through multiple steps. Thus, the highly efficient and clean technologies for these sectors are necessary for saving energy and reducing CO_2 emission (Pak et al., 2010). Among the alternative means, fuel cell technologies have been attracted because they can transform directly the chemical energy of fuel into electricity and emit clean exhaust gases.

Fuel cells have been developed for a long time since the principle of fuel cell has demonstrated by Sir Groove at 1939, who suggested the "gas battery" (Andujar & Segura, 2009). Initially, fuel cells were seen as an attractive technology for the generation of power due to high theoretical efficiency. However, as the efficiency of other alternative technologies was rapidly being increased, the development of fuel cell became almost negligible during the early of 20^{th} century (Perry & Tuller, 2002). Also, since the interest in fuel cell reoccurred by the "space race" between USA and Russia in the late of 1950s and the first actual power generation system of fuel cell was launched in the Gemini at 1962, many types of fuel cells were developed for many applications and categorized by the electrolyte for use.

Among the various kinds of fuel cells, polymer electrolyte fuel cells (PEFCs) have extensively been developed for transport and distributed-power generation applications due to low

emission of GHG and high efficiency compared to the internal combustion engine (ICE) and generators. Thus, PEFC technology is considered as a green technology for energy savings and reduction of GHG emission. As a one part of PEFCs, direct alcohol fuel cell (DAFC), which can use the high energy density of alcohol such as methanol and ethanol that could be produced by using the biomass and corn for carbon neutral cycle or directly using solar energy for artificial photosynthesis, is the most promising fuel cell for mobile and portable applications.

Although the PEFC systems have been developed to its current status through several technical breakthroughs over the years, it is now on initial market stage with the help of government for new and renewable energy policy. To expand the market size or thrive in fuel cell market without external supports, further innovations in the areas of cost and durability are demanded. For this innovation, the understanding and improvement of materials and components for membrane electrode assembly (MEA), which considered as the core of fuel cell system, are very important besides development of fabrication process maximizing the performance with the improved materials for PEFC.

A typical MEA as shown in Fig. 1 consists of a polymer electrolyte membrane (PEM), interposed by two electrodes, cathode and anode, which are composed of catalyst layer (CL) and the gas diffusion layers (GDL), respectively. Usually, a microporous layer (MPL) made from porous carbon materials is located between the CL and the GDL. The total thickness of multilayer of MEA is less than 500 μm (Ramasamy, 2009).

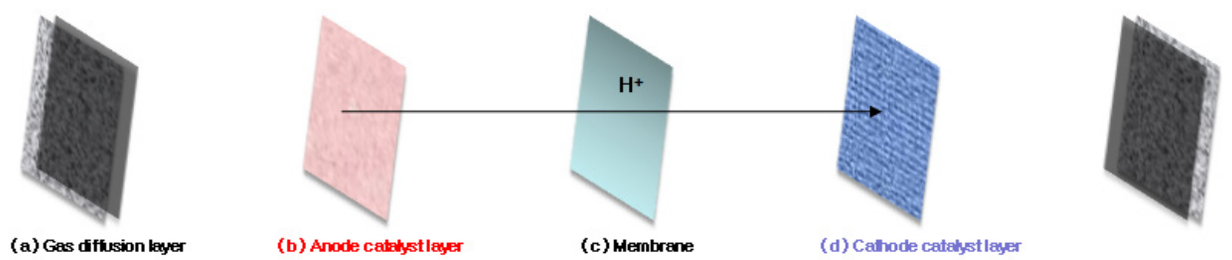

Figure 1. Schematic components of a membrane electrode assembly

The performance of MEA is displayed by the power density (W/cm^2), which is the product of current density (A/cm^2) and voltage (V), which is totally dependent on the choice of components and materials, especially membrane and catalyst. Thus, the research for increasing the performance of MEA is usually focused on the new materials for membranes and catalysts with enhanced properties. However, to reveal the improved performance of materials in the MEA level, the fabrication process for MEA should be optimized.

In this chapter, the processes for MEA preparation are reviewed in the section 2 and the optimized performance of MEA using new supported catalysts will be discussed in the sections 3 and 4. Finally, the chapter is closed with conclusions.

2. Processes for membrane electrode assembly (MEA)

Among the components of a MEA, the performance of the MEA is usually dependent on the CL properties and contact interfacial resistance between the CL and membrane according to

its preparation technique. The CL has its own set of criteria to fulfil the chemical reaction with complex functionalities and has a three-dimensional porous structure composed of a network of catalyst particles made of porous carbon supports and catalytic metal nanoparticles, usually and ionomer fragments.

Some common requirements of an idea regarding to CL must have a high electrocatalytic activity for PEFC reactions, a good ionic transport and a high porosity for efficient transport reactant and product (Ramasamy, 2009). Over the years, various slurry formations and coating procedures have been developed for the preparation of CLs in order to realize the better performance of MEA for the commercialization.

One key factor in the preparation of CLs is the selection of solvents to form a homogeneous mixture in the catalyst ink, which was generally made by dispersing the catalyst (supported Pt based catalyst or Pt based black catalyst) with a mixture of Nafion ionomer solution, the solvents and deionized (DI) water. Many researchers have mainly studied to focus on the dispersion of catalyst ink formed by ionomer and the catalyst particles. For example, Uchida et al. demonstrated that the further improvement in cell performance could be obtained by using an intermediate dielectric constant solvents with a range of 3 -10 to form a colloidal suspension of Nafion particles in a water-alcohol mixture. Their experimental results were attributed to the higher number of electrochemical interactions between the Nafion ionomers and catalysts in the extended reaction interface than those using solvents with a high-dielectric-constant, such as water (Uchida et al., 1998). It is suggested that the selection of highly viscous glycol for the catalyst ink as a solvent resulted in the higher performance MEAs in which showed low mass-transfer and electrode ionic resistance due to the formation of homogeneous catalyst particles in the catalyst ink (Wilson et al., 1995). Although the homogeneous ionomer and the catalyst particles are important for the formation of the slurry ink, the appropriate amount ratio of ionomer to catalyst and fine distribution of the ionomer in the CLs are the most critical factor, which leads to the minimized electrode resistance and maximized contact of ionomer with catalytic metal nanoparticles. This ratio should be normally optimized for the best formulation of the catalyst ink.

Another key factor in preparation of the CLs is the selection of coating procedures to minimize the roughness factor of the CLs and the contact resistance between the CL and the membrane. The types of coating procedure for preparation of the CLs can be broadly classified into three categories as followings: (1) catalyst coated on electrode (CCE), (2) decal transfer catalyst coated on membrane (DTM) and (3) direct catalyst coated on membrane (DCM).

2.1. Catalyst coated on electrode method (CCE)

The CCE method is to form the CL on the GDL as shown in Fig. 2. The catalyst ink was coated onto the MPL in the GDL, and then the electrode was dried in the vacuum oven at a specific temperature. Finally, the MEAs were assembled by hot pressing the catalyst coated electrodes with a membrane. The CCE method has widely been used in the formation of the

large scale mass production of MEAs due to the simple coating process (Frey & Linardi, 2004). The final hot-pressing is indispensable and important process for the higher performance MEA to make a good interfacial contact between the CLs and membrane in the CCE Method. The main parameters of hot-pressing process are the temperature, the pressure and the time. Zhang et al. investigated that the effect of hot-pressing conditions (temperature, pressure and time) on the performance of MEA using the CCE method for the DMFC. The optimized parameters for temperature, pressures and time are 135℃, 80kg_f/cm^2 and 90s, respectively. The highest power density of MEA is attributed to the lowest contact resistance between the membrane and CL (Zhang et al., 2007). In addition, Therdthianwong et al. tried to find systematically the most significant hot-pressing parameter by designing a full factorial analysis of the three main hot-pressing parameters related to the cell performance (Therdthianwong et al., 2007). In this study, MEA prepared with hot-pressing condition of 100 °C, 70.3 kg_f/cm^2 and 120s resulted in the highest power density.

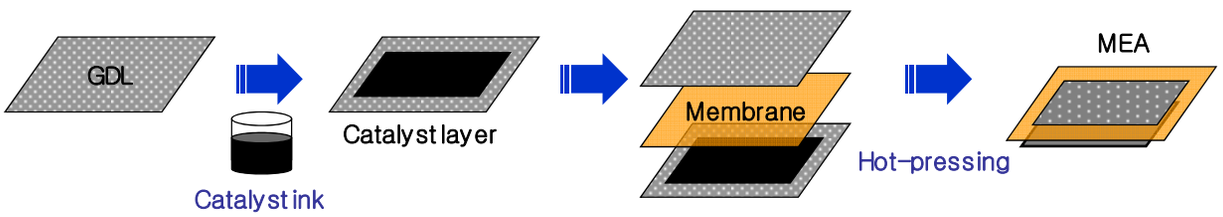

Figure 2. Schematic process of a catalyst coated on electrode (CCE).

Although various conditions for hot-pressing have been employed by researchers in the CCE method, the controlling of hot-pressing temperature to slightly above the glass transition temperature of the membrane might be a critical point to promote good contact within the triple-phase regions of the CL. (Zhang et al., 2007, Tang et al., 2007, Lindermeir et al., 2004). However, the CL prepared in CCE method cannot be effectively transferred to the membrane during the course of hot-pressing the MEA due to the change of the structure in the CL (a distribution of ionomer and porosity) and the dehydration of the membrane, which may lead to an irreversible performance loss of the MEA (Kuver et al., 1994).

2.2. Decal transfer catalyst coated on membrane method (DTM)

The DTM method is to form the CL on the decal substrates as a shown in Fig. 3. The catalyst inks were coated uniformly onto decal blank substrates. The CLs of both electrodes were then transferred from substrates to the membrane by hot pressing under high pressure and temperature for a specific time. The decal substrates can be peeled away from the CCM leaving the CLs fused to membrane, yielding a three-layer CCM. The GDLs can then be added to the CCM by hot-pressing as mentioned in the previous section.

Tang et al. reported that the DTM method could show a better utilization of catalysts and a superior formation of the ionomer network compared to the CCE method, which are all beneficial for improving the performance and long-term durability of the MEA for the DMFC due to a low interfacial resistance between the CL and polymer membrane, a thinner catalyst layer with a lower mass transfer resistance, and a better contact among the electrode

components (Tang et al., 2007). However, the process of the DTM method seems to be more complex than CCE method and impossible to control the porosity and the thickness of the CLs due to the dehydration of the membrane during the decal transfer and, it has a possibility of sintering of the catalytic nanoparticles (Song et al., 2005). Furthermore, the ionomer segregation is likely to occur onto the outside of the CL during the transfer step of the CLs from the decal substrates to Na^+-Nafion membrane with high hot-pressing temperature in order to increase the transfer ratio of the CL into the membrane (Xie et al., 2004). Recently, a breaking layer composed of carbon powder and Nafion ionomer on the CLs was suggested by two groups to overcome those problems, that is, the CL was sandwiched between the inner thin carbon and the outer ionomer layers (Park et al., 2008, Cho et al., 2010). However, the additional layer could generate a further resistance to proton and mass transports, which may lead to an irreversible performance loss of the MEA. The DTM method must be improved further for the commercialization of MEA.

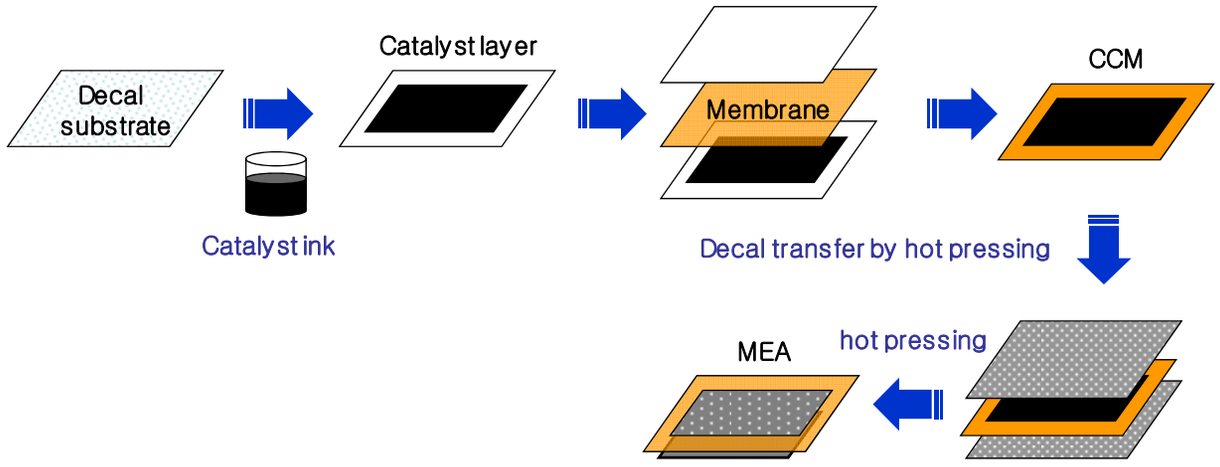

Figure 3. Schematic process of a decal transfer catalyst coated on membrane (DTM)

2.3. Direct catalyst coated on membrane method (DCM)

The DCM method is to form the CL directly onto the membrane as shown in Fig. 4. The DCM method is more simple and efficient than indirect coating process, DTM method and has no risk of uneven and incomplete transfer of catalyst in the CL. Furthermore, it also produces a higher MEA performance than the DTM method due to an easier controllability of the CL thickness as well as a better ionic connection between the CLs and the membrane resulted from a strong attachment of the solvent on the membrane. However, the direct coating of catalyst slurry onto the membrane has a critical problem that the membrane has a

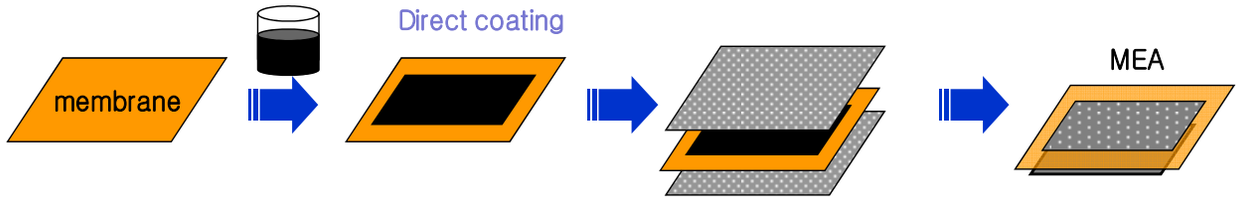

Figure 4. Schematic process of a direct catalyst coated on membrane (DCM)

high tendency to swell or wrinkle with a contact of many solvents in the catalyst slurries, which could give rise to the deformation of the CL by fast volume changes of the membrane.

It could cause the membrane and the CL to be deformed by fast volume changes. Therefore, swelling control of the membrane is very important in the DCM method for the high quality MEA fabrication. To minimize such dimensional changes during the catalyst coating process, many researchers have tried to prevent the membrane from swelling during the coating process. For example, Park et al. suggested a process by employing a pre-swollen Nafion membrane. They soaked the Nafion membrane in EG and sprayed the catalyst slurry onto the pre-swollen membrane. Thus, the prepared MEA showed improvement over a commercially available MEA due to the reduction of a stress problem of membranes by the pre-swelling process (Park et al., 2010). Shao et al. prepared MEA using direct spray deposition of the catalyst ink into Nafion 212 membrane with the aid of a hot-plate at 150 °C, whose condition could decrease the swelling and wrinkling of the Nafion membrane due to the solvent gasification before being absorbed into the Nafion membrane (Shao et al. 2001). Also, in case of our lab, an innovative process preventing the swelling from the solvents by holding a membrane on a porous vacuum plate is developed, which is an efficient way for realizing a high precision in catalyst loading with high reproducibility (You et al. 2010). Considering the CL design, the selection of good solvents and DCM method as a coating process could offer a more efficient and attractive way for high quality and high performance of MEAs.

3. Optimization of DCM processes for MEA

One parameter in MEA design to improve the performance of DMFCs is to increase the catalyst utilization and electrochemical surface area (ESA) of the electrodes by increasing the level of gas access, proton access and electron access to the reaction sites. Hence, the structures of CLs where the electrochemical reactions occur should be optimized for maximizing the triple-phase boundaries. In addition, minimizing a resistance between the catalyst and ionomer in the CL, as well as the interfacial resistance between the electrolyte and the CL are essential in MEA structure. Furthermore, the resistance of the electrolyte membrane itself should be minimized.

Another parameter in MEA design is the control of porosity to maximize their active surface area of catalyst in the electrodes. During DMFC operation, complex flow of reactants and reaction products exists in the porous space of CL. The pores in cathode should allow oxygen to reach the catalyst surface and support efficient transport of water to prevent flooding of the layer. One method achieving a good balance of fuel transport capability with effective product removal is the addition of pore-forming materials into the CL. They help tailor the CL morphology and pore structure to meet the above-mentioned requirements, thereby decreasing the transport resistance.

Considering the above-mentioned issues in the CL design, the optimized design of CLs must have the lowest resistance between the membrane and CL, the proper distance of proton conductor from the catalyst and the optimum porosity of the catalyst layer. The

DCM method with the catalyst slurry composed of EG and pore forming agent is investigated to optimize the structure of CLs by parameters for hot-pressing such as temperature and pressure.

3.1. Preparation of electrode and MEA

All investigated MEAs in this section were prepared with the hydrocarbon membrane (the conductivity and thickness of the membrane was 0.06 S/cm and 32 μm, respectively) and the SGL 25 BC for GDLs of both electrodes. Pt-Ru black (HiSpec 6000, Johnson Matthey) and Pt black (HiSpec 1000, Johnson Matthey) were used as the anode and cathode catalyst, respectively. Catalyst inks, consisting of black catalysts, Nafion solution, DI water, $MgSO_4$, and EG with weight ratios of 0.288: 0.18: 0.155: 0.058: 0.36 for the anode and 0.241: 0.151: 0.12: 0.036: 0.452 for the cathode, respectively, were well dispersed using high speed rotating equipment (conditioning mixer, AR-500) for 10 min.

For the preparation of CLs using the DCM, the anode inks were coated uniformly onto one side of the electrolyte membrane directly, which was held on a vacuum plate with 32 mm × 32 mm mask films to prevent dimensional change of the membrane. The coated membrane was then dried for 24 h in a vacuum oven at 120ºC after removing the mask. The cathode catalyst ink was applied to the opposite side of the anode-catalyst coated membrane in the same manner. The catalyst loading for both electrodes was 5 mg/cm^2 and the active area of the MEAs was 10 cm^2.

Hot-pressing after direct coating of CL was performed at three different temperatures (140, 150, and 160ºC) and pressures (0.1, 0.2, and 0.3 ton$_f$/cm^2) for 10 min to control the porosity and contact resistance of the CLs. And then, The CCM prepared was pre-treated in a solution containing 1M methanol and 1M sulfuric acid at 95ºC for 4 h. Finally, the MEAs were fabricated by placing GDLs onto the corresponding sides of the CCM by hot-pressing at the 125ºC and 0.1 ton$_f$/cm^2 for 3 min.

The performance of the MEA under the DMFC condition was measured by fuel cell testing system (Won-A Tech) using single cell hardware with an active area of 10 cm^2. A 1M aqueous methanol solution was fed to the anode side at a flow rate of 0.25 ml/min·A. Dry air was supplied to the cathode side at a flow rate of 45 ml/min·A under ambient pressure. The cell performance was measured at 60ºC and operated in potentiostatic mode at a voltage of 0.45V for 4 h each day. The polarization curves of the MEAs were recorded at the end of the procedure at a constant voltage.

Electrochemical impedance spectroscopy (EIS) of the MEAs were measured at a current of 220 mA/cm^2 using an electrochemical analysis instrument (VMP2) in the frequency range from 100 kHz to 0.1 Hz with 10 points per decade at 60 ºC. The amplitude of the sinusoidal current signal was 10 mA. To separate the anode and cathode impedance, the cathode side was supplied with a continuous supply of hydrogen, which would function as a dynamic hydrogen reference (DHE) and counter electrode.

3.2. Effects of the temperature for the hot-pressing

The effect of the hot-pressing conditions (temperature and pressure) on the MEA performance for DMFC was investigated to decrease the reaction transfer resistance through the extended catalyst and ionomer interface in the electrode and to increase the interfacial bonding through the strong formation of a proton conducting ionomer network between the CL and membrane. Fig. 5 (a) shows the power densities at 0.45V of the MEAs from the CCMs prepared by the DCM at various hot-pressing temperatures under the same pressing pressure (0.2ton$_f$/cm^2). The performance of the MEA produced at a hot-pressing temperature of 150 ºC was higher than that of the MEA produced at 140 and 160 ºC, respectively.

Electrochemical impedance spectroscopy (EIS) and differential scanning calorimetry (DSC) were performed to elucidate the effect of the hot-pressing temperature on the DMFC MEA performance. Firstly, in EIS analysis, the reaction transfer resistance of the anode, cathode, and the total showed similar values regardless of the hot-pressing temperature, as shown in Fig. 5 (b). This indicates that the pressing temperature for CLs is not related to the reaction transfer resistance between catalyst and ionomer, and pore structure but is associated with changes in the interfacial properties by the strong bonding between the CL and membrane. Secondly, Fig. 5 (c) shows the DSC analysis of the hydrocarbon membrane. The exothermic process was observed at 150 °C, which corresponds to the glass transition temperature (Tg) of the hydrocarbon membrane. At an appropriate temperature, such as 150 °C, side chain movement brings the -SO_3H group out of the bulk to the surface to decrease the surface energy (Liang et al., 2006, Guan et al., 2006, Robertson et al., 2003). This might give rise to intimate bonding between the hydrocarbon membrane and CL resulting in the enhanced proton conductivity. Therefore, the optimum hot-pressing temperature contributes to the significant increase in the MEA performance.

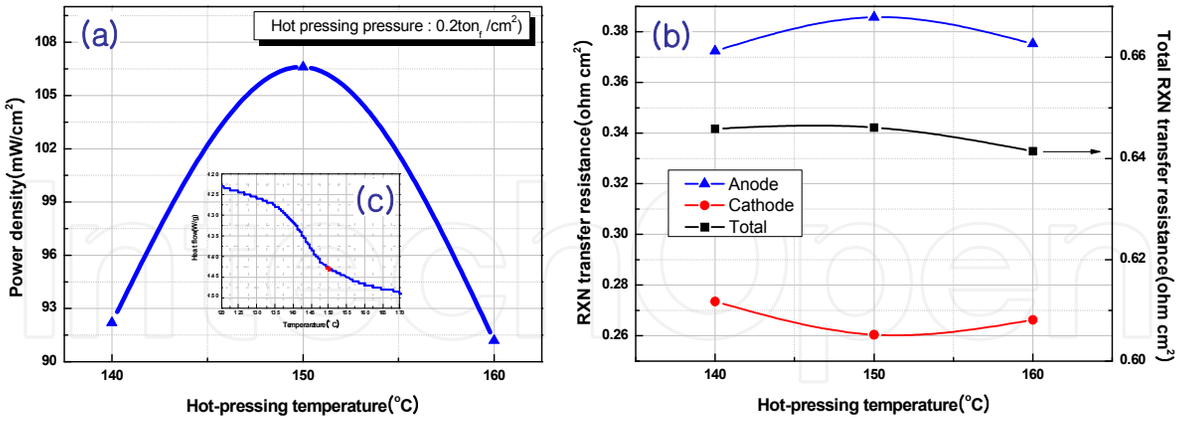

Figure 5. Effect of hot pressing temperature for the CCM prepared by direct coating on (a) power density of MEA and (b) reaction (rxn) transfer resistance from electrochemical impedance spectroscopy (EIS) and (c) DSC analysis of hydrocarbon membrane.

3.3. Effects of pressure for the hot-pressing

Fig. 6 (a) shows the power densities at 0.45V and reaction transfer resistances of the MEA using CCM produced by the DCM under various hot-pressing pressures under the same

temperature of 150 °C. The increase of hot-pressing pressure for the CCM to approximately 0.225ton$_f$/cm^2 resulted in significantly improved MEA performance with power density up to 107mW/cm^2 at 0.45V and 60 °C. This might be attributed to the decreased reaction transfer resistance by the improved proton conduction and oxygen transport through the well-connected network of the CLs in the MEA. However, further increases in the hot-pressing pressure led to a decrease in the performance of MEA owing to the destroyed microstructures of the CL by excessive pressing.

This suppose was confirmed by EIS analysis of the MEAs. Fig. 6 (b) shows the effect of the hot-pressing pressure for the CCM prepared by DCM on the reaction transfer resistance. The cathode reaction transfer resistance increased as both CLs were further compressed by increasing the hot-pressing pressure, whereas the anode reaction transfer resistance decreased, even though the thickness of both CLs have decreased. Generally, the thickness of both porous CLs decreases with increasing of density (decreased porosity) as the pressing pressure increases to fabricate the CCM. The dense anode CL may increase the methanol utilization efficiency with the decreasing of the methanol crossover, resulting in the decreased the anode reaction transfer resistance. This phenomenon might be that because the dense anode CL serves as an additional resistance against methanol crossover (Mao et al., 2007, Liu et al., 2006, Park et al., 2008). In contrast, the thick microstructure (high porosity) for the cathode CL is essential for transporting reactant gas effectively from the GDL to CL and for eliminating the water produced by the electrochemical reaction from the CL to GDL (Liu & Wang, 2006, Wei et al., 2002, Song et al., 2005). Therefore, the hot-pressing pressure for the CCM showed the lowest total reaction transfer resistance at 0.2 ton$_f$/cm^2 and resulted in the highest power density of the MEA produced by the DCM. It was suggested that the hot-pressing condition has a significant effect on the electrochemical performance of MEAs, particularly in the reaction transfer resistance.

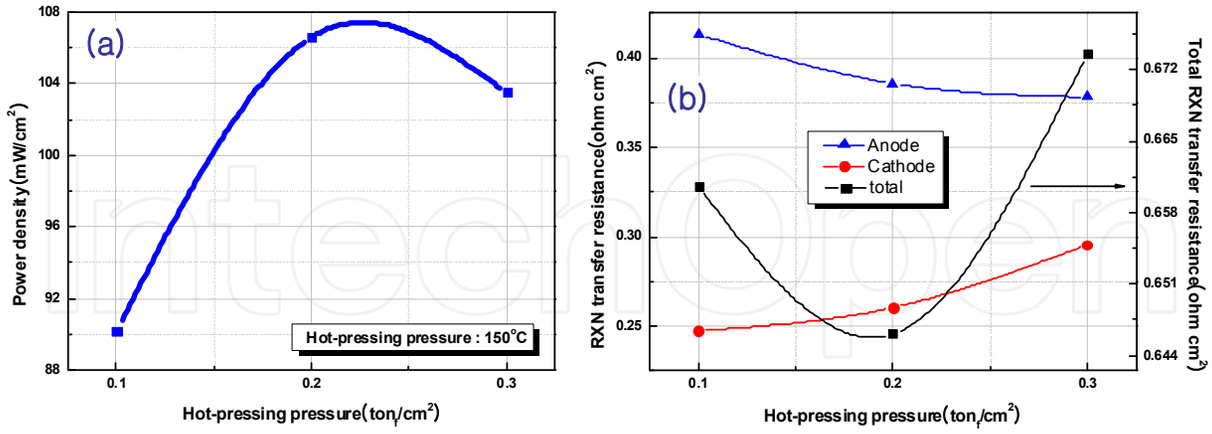

Figure 6. Effect of hot-pressing pressure for the CCM prepared (a) power density of MEA and (b) reaction (rxn) transfer resistance from EIS.

3.4. Effect of pore forming agent in the cathode

The magnesium sulphate ($MgSO_4$) was chosen as a pore forming agent for the preparation of the cathode CL. The $MgSO_4$ is widely used as a drying agent due to its hygroscopic

properties (readily absorbs water from the air). Hence, it can be easily removed in the CL by boiling the CCM at DI water after DCM process. The vacant sites in the CL by resulted from removed $MgSO_4$ may play a role as pores. In addition, compared to that of insoluble pore forming agents (e.g. Li_2CO_3) (Tucker et al., 2005), the addition of soluble $MgSO_4$ could form more uniform pore distributions with smaller pore size (approximately 3 nm as a shown in Fig. 7 (b)) in the CL by the homogeneous catalyst inks, since the solubility of $MgSO_4$ was superior in catalyst ink mixtures composed of the water, EG, ionomers and catalysts.

Fig. 7 (a) shows the effect of the pore forming agent ($MgSO_4$) loading in the CL on the power density of the MEA by the DCM. As it can be seen, the addition of $MgSO_4$ in the catalyst slurry from 0 wt% to 30 wt% led to an increase in power density of MEAs at 0.45V. This might be due to the higher degree of catalyst utilization and increase in active ESA because more pores that had formed by the $MgSO_4$ contributed ~~to~~ the supply of air to the catalytic active sites effectively to produce the required amount of power, and eliminate the water produced by the electrochemical reaction. Moreover, the effect of the cathode reaction transfer resistance by the addition of $MgSO_4$ showed an opposite trend to the result of the cell performance as shown in Fig. 7 (a). However, further increasing of $MgSO_4$ showed an increase of cathode reaction transfer resistance due to the destroyed microstructures of the weaken CL mechanically by excessive porous structure. Furthermore, the resistance for the proton transport to and from the active sites increased with increasing distance between catalysts and ionomers at the CL. Therefore, the pores generated by the $MgSO_4$ might be an effective channel for air transport inside the CL. In addition, increased pore volumes are expected to enhance rapid mass-transfer near the catalyst surface providing open diffusion paths for the water produced from the CL. Furthermore, the enhanced oxygen supply increased the rate of oxygen reduction because the charge transfer reaction is a function of the reactant concentration.

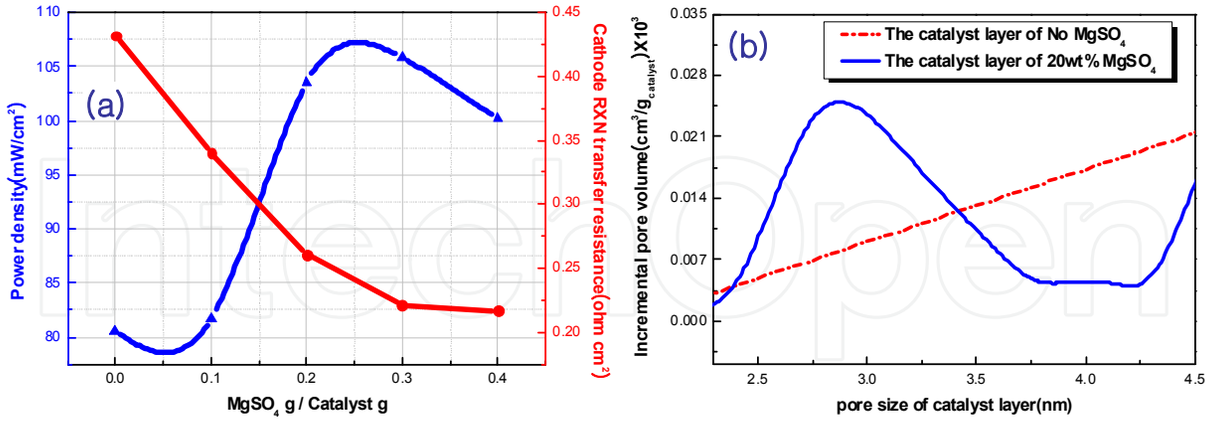

Figure 7. Effect of $MgSO_4$ amount in the catalyst layer of CCM prepared on (a) power density and cathode reaction transfer resistance and (b) pore size distribution of catalyst layer.

4. High performance MEA using new supported catalyst

In this section, the adoption of new supported catalyst (Pt/OMC) consisted of novel ordered mesoporous carbon (OMC) support and highly dispersed Pt to the cathode catalyst layer of the

MEA for DMFC is presented as an example of optimization of properties such as catalyst loading, ionomer concentration and porosity in the electrode (Kim et al., 2008). The Pt/OMC catalysts have been developed in our lab over several years for the DMFC, which is based on the novel OMC supports having very high surface area and ordered array of mesopores inside the particles (Chang et al., 2007, He et al., 2010, Joo et al., 2009., Lee et al., 2009, Pak et al., 2009).

A balance between proton conduction path and mass transport via pore structures of catalyst layer was investigated by changing an amount of ionomer and compressing the MEA with hot press. The performance of MEA as a function of voltage was measured to determine the optimized the conditions for catalyst layer, which governs the power density. Furthermore, the performance of MEA with optimized Pt/OMC catalyst layer was compared to that of unsupported Pt black catalyst layer to prove the possibility for decreasing the Pt amount in the cathode without loss of power density for DMFC.

4.1. Characteristics of OMC support and Pt/OMC catalyst

The SEM and TEM images of ordered mesoporous silica (OMS), which is the hard-template for OMC, and OMC were displayed in the Fig 8. As observed in Fig. 8, the OMS is composed of 200 – 300 nm particles and OMC has similar particle morphology and size, which indicates that the nano-replication (Joo et al., 2001) of OMS into OMC is successfully occurred and the removal of OMS to generate the pore inside of the OMC did not alter the apparent morphology of OMC. The TEM image from OMS (Fig. 8 (b)) shows that the uniform mesopores are hexagonally well-arranged in the particle. For the OMC, the TEM image display that the pores and the walls of OMS are inverted to the carbon-nanorod and mesopore of OMC, respectively. The low angle X-ray diffraction (XRD) patterns (refer to Joo et al., 2006) of OMS and OMC showed three, well resolved peaks corresponding to (1 0 0), (1 1 0) and (2 0 0) diffractions of hexagonal p6mm symmetry. The unit cell dimension of OMS and OMC, estimated from the (1 0 0) diffraction was 12.0 and 11.0 nm, respectively. The OMC has a slightly compressed unit cell because of the structural shrinkage of carbon frameworks during the high temperature carbonization (Jun et al., 2000).

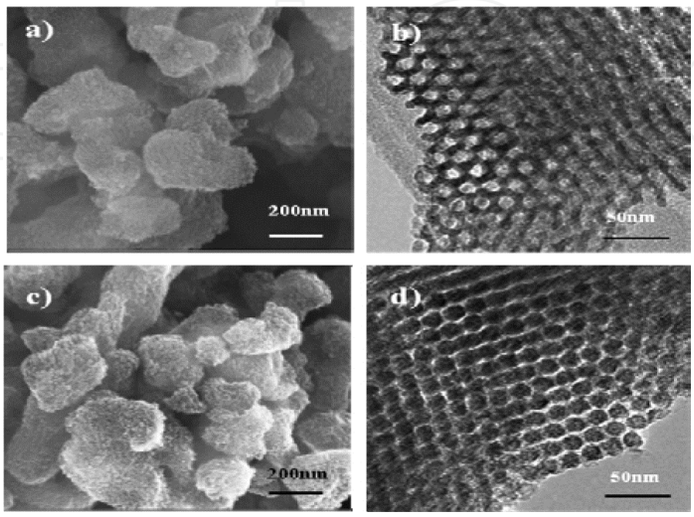

Figure 8. SEM and TEM images of (a, b) OMS and (c, d) OMC, respectively.

The pore structures of OMS and OMC were further characterized by using the nitrogen adsorption and desorption isotherms (Joo et al., 2006). The corresponding pore size distribution estimated from the adsorption branch by BJH method for OMS and OMC samples. The OMS template showed typical Type IV isotherm with H1 hysteresis. The sharp increase of nitrogen uptake in the adsorption branch in the partial pressure of 0.8–0.9 indicates that the mesopore of OMS has uniform distribution through the particles. The BET surface area of OMS template is 451 m^2/g and pore volume is 1.27 cm^3/g, while the pore diameter calculated from the adsorption branch of isotherms is 12.2 nm. The nitrogen isotherms of OMC sample exhibited similar shapes, where capillary condensation occurred in the partial pressure range of 0.4–0.6. The BET surface area of OMC sample is 884 m^2/g and pore volume is 0.86 cm^3/g, while the pore diameter is 4.0 nm.

The unique structural characteristics of OMCs make them suitable as catalyst supports for DMFC application as mentioned earlier. For example, the high surface area of OMC, compared with the conventional carbon blacks such as Vulcan XC-72R and Ketjen Black, can provide sufficient surface functional groups or anchoring sites for the nucleation and growth of metal nanoparticles, thus metal catalysts can be prepared on OMC with high dispersion. Further, uniform mesopore structure of OMC would facilitate the diffusion of reactive molecules for electrochemical reactions.

Pt nanoparticles were supported on the OMC by incipient wetness impregnation of the Pt precursor ($H_2PtCl_6 \cdot xH_2O$) in acetone solution into the pores of OMC support and subsequent reduction under H_2 flow. The total loading of Pt was controlled as high as 60 wt%, because an electrocatalyst for DMFC application requires very high metal loading (Chang et al., 2007). The TEM image of Pt/OMC (Fig. 9 (a)) indicates that Pt nanoparticles are uniformly scattered on the carbon nanorod of OMC. The average particles size determined from the TEM image is 2.85 nm. The XRD patterns for 60 wt% Pt/OMC presented in Fig. 9 (b) showed distinct peaks at around 39.8°, 46.3° and 67.5°, corresponding to the (1 1 1), (2 0 0) and (2 2 0) planes of a face-centered cubic structure, respectively. The crystalline size of the Pt nanoparticle estimated by the Scherrer equation is 2.86 nm, which is matched well with the value obtained from TEM analysis.

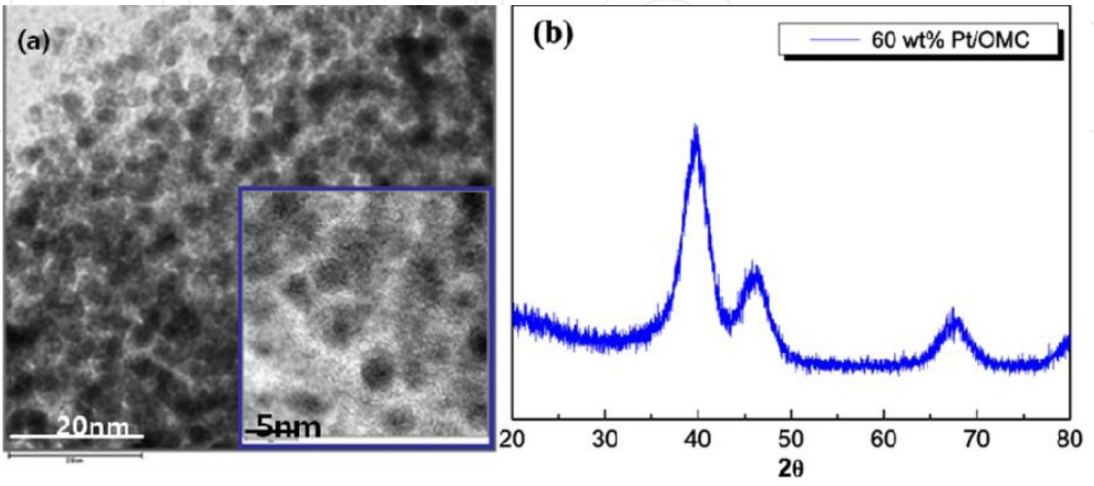

Figure 9. (a) TEM image and (b) XRD pattern for Pt/OMC catalyst.

4.2. Optimization of catalyst layer with Pt/OMC catalyst

To realize the adoption of Pt/OMC in the cathode catalyst layer for DMFC, the effect of the ionomer contents (18, 30 and 45 % compared to the Pt/OMC) and process parameter (compressed vs. uncompressed) were investigated on the morphology of electrode and performance of MEA at 70 °C as summarized in the Table 1. The catalyst ink was sprayed directly on to a Nafion 115 membrane to form the so-called CCM. The membrane was held on a vacuum plate to prevent dimensional change of the membrane during the direct coating of the ink. The cathode catalyst ink was coated on one side of the membrane followed by drying at 60 °C under vacuum for 2 h. On the uncoated side of the cathode-coated membrane, the anode catalyst ink was applied in the same manner. As a reference, the catalyst layer based on unsupported Pt black catalyst (Johnson Matthey, HiSpec® 1000) at a loading level of 6mg/cm^2 was also prepared. The geometric area of the catalyst layers was 25 cm^2. In order to produce a catalyst layer with lower porosity, the cathode-coated membranes were compressed at 30 MPa and at 135 °C for 5 min before the subsequent anode coating was performed. As a diffusion layer, 35 BC (SGL, Germany) was used for both the cathode and the anode. The MEAs were prepared by hot pressing the CCM and two diffusion layers at 125 °C and 51 MPa. The morphology of the catalyst layers was observed by SEM.

Catalyst Layer	Amount of Pt (mg/cm^2)	Ionomer content (%)	Compression
CL18-U	2.39	18	X
CL18-C	2.39	18	O
CL30-U	2.64	30	X
CL30-C	2.64	30	O
CL45-U	2.39	45	X
CL45-C	2.39	45	O

Table 1. Physical parameters of catalyst layers based on Pt/OMC catalyst

The thickness of the uncompressed catalyst layers (CL18-U, CL30-U and CL45-U) is 70, 128 and 132μm, respectively, for corresponding ionomer contents of 18, 30 and 45 % and the thickness of the compressed catalyst layers (CL18-C, CL30-C and CL45-C) is found to be 64, 53 and 48% of the pristine thickness for ionomer amount of 18, 30 and 45%, respectively. In the case of ionomer amount of 12%, the strength of catalyst layer is not enough to adhere on the GDL, which could be attributed that the ionomer content is not enough to bind Pt/OMC catalysts effectively. The ionomer contents become more than 12% and the catalyst layer showed acceptable mechanical strength.

The apparent shape of the Pt/OMC-based catalyst layers was observed by SEM, as displayed in Fig. 10 for representative examples (CL18-U and CL18-C). These are featured by the formation of agglomerates of the Pt/OMC and ionomer and of the pores between these agglomerates. The agglomerate size is in the range of 200–1000 nm. Considering the size of

the primary OMC (200–300 nm) particle as shown in Fig. 8, several Pt/OMC particles are included in the agglomerate. The change of ionomer amount did not cause the appreciable changes in the size of the agglomerates in the catalyst layers. For the uncompressed catalyst layers, the porosity appears to be larger at higher ionomer contents.

After compression, densification of the catalyst layer is observed. On the other hand, the size of the agglomerates is little affected by the compression, as shown in Fig. 10. This indicates that macropores between the agglomerates are reduced during the compression process. The compressed catalyst layers do not differ in their pore structures.

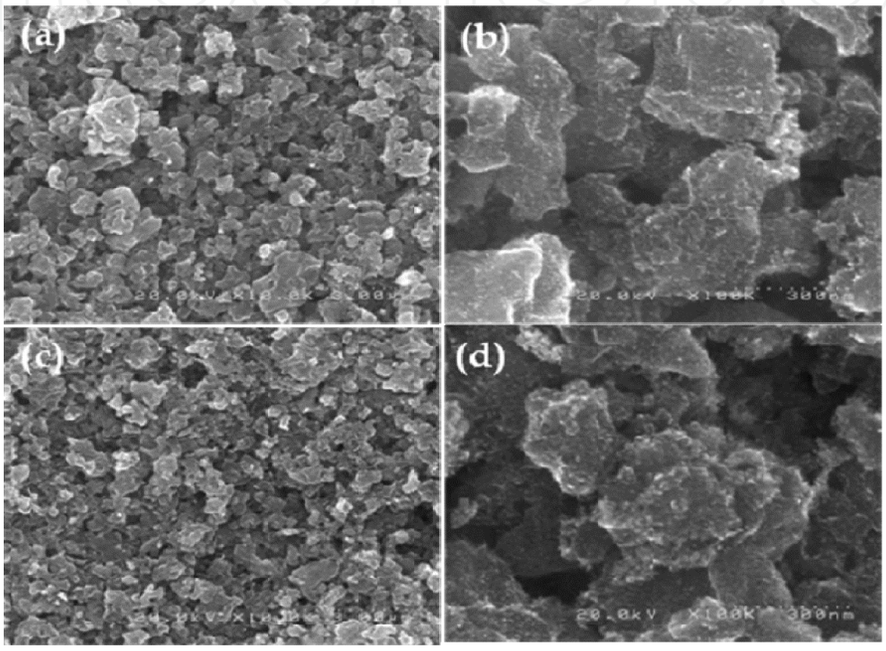

Figure 10. Represnetative SEM images with different magnification of (a, b) CL18-U and (c, d) CL18-C.

Fig. 11 showed polarization curves obtained after five day activation at 70 °C. Among the MEA, CL18U-C case showed the highest power density of 104.2 mW/cm² at 0.45 V. The operating voltage of DMFC MEA was chosen based on the balance between power density and energy efficiency. Operation at lower voltage generates high power density, and thus size reduction of the stack is possible. On the other hand, energy efficiency decreases on lowering the voltage, which requires a larger fuel tank for a given energy consumption. To maximize the system efficiency, an operating voltage of 0.45V is chosen for DMFC usually. Dry air and 1M aqueous methanol solution were used as feed stocks for the cathode and the anode, respectively. As shown in Fig. 11, uncompressed MEAs show higher performance at 0.45 V than that of compressed MEAs with same amount of ionomer in the catalyst layer. The variation of the ionomer amount results in a more pronounced effect on the power density than compression of catalyst layer, which is consistent with a result reported earlier in the literature (Frey and Linardi, 2004). As the catalyst layer compressed, the layer becomes more compact, which reduced the mass transport in the catalyst layer. However, the proton conductivity in the catalyst layer should be increased with compression, which was confirmed by the analysis of impedance (Kim et al., 2008).

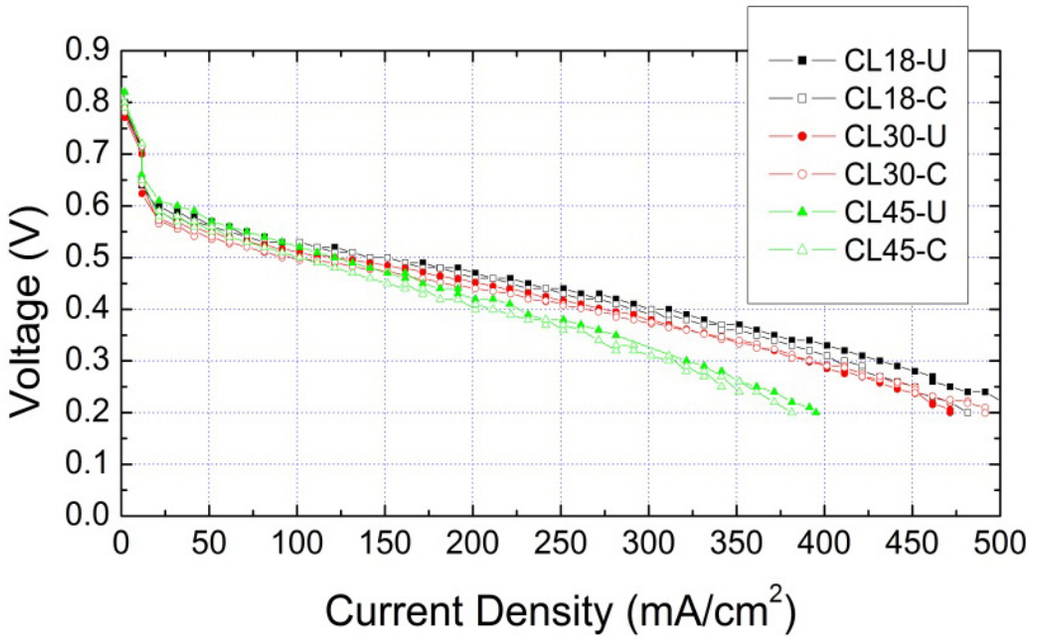

Figure 11. Polarization curves for MEAs based on Pt/OMC at 70 °C (cathode feed: air, anode feed: 1M CH_3OH).

Thus, the decrease in power density with the compression indicates that mass transport is more important than the proton conductivity (ionic transport) for the Pt/OMC based cathode. A similar finding was reported for a PtRu/C supported catalyst in the previous paper, which suggested the compaction of the anode catalyst layer led to a decrease in performance by 23% due to increased mass transport (Zhang et al., 2006).

For both the uncompressed and compressed MEAs, the gap of power density increases with reducing in the ionomer content above 150 mA/cm^2. Below 150 mA/cm^2, however, the difference is less pronounced, where the power density of CL45-U becomes comparable to that of CL18-U. The large difference in power densities at high current densities indicates a considerable mass-transport limitation at higher ionomer amount. When conventional Pt-supported carbon is used, there is an optimum value of ionomer content in the catalyst layer to obtain the best performance. Even though the existence of an optimum at lower ionomer content is expected for a Pt/OMC-based catalyst layer, it is not possible to confirm this

because the mechanical integrity of the catalyst layer is not sufficient as mentioned earlier in this section. An improvement in the formation of the three-dimensional network of the ionomer phase which provides mechanical integrity is needed to confirm the existence of an optimum at lower content of ionomer.

The polarization behaviour of a CL18-U catalyst layer at a loading level of 2 mg/cm^2 and a catalyst layer based on Pt black catalyst at a loading of 6mg/cm^2 is compared at Fig. 12. The thickness of the catalyst layer for the CL18-U and Pt-black catalysts is 70 and 45 μm, respectively. The MEAs have identical components, except the cathode catalyst layer. The CL18-U catalyst delivers higher power at high voltages (>0.4 V) and lower power density at low voltages (<0.4 V) than the Pt black-based cathode. Since catalytic activity governs the electrochemical reaction rate at the high voltages (activation region), the higher power density for Pt/OMC indicates that 2 mg/cm^2 of Pt/OMC gives higher catalytic activity than 6 mg/cm^2 of Pt black catalyst, which is of practical importance. With the introduction of an OMC support, the Pt loading in the cathode can be reduced to one-third of Pt black-based catalyst layer, without any negative effect on power performance, and this would significantly contribute to cost reduction of MEAs. The lower power density for the Pt/OMC catalyst layer at high-current density indicates that the mass-transport limitation is greater than that for the Pt black-based catalyst layer.

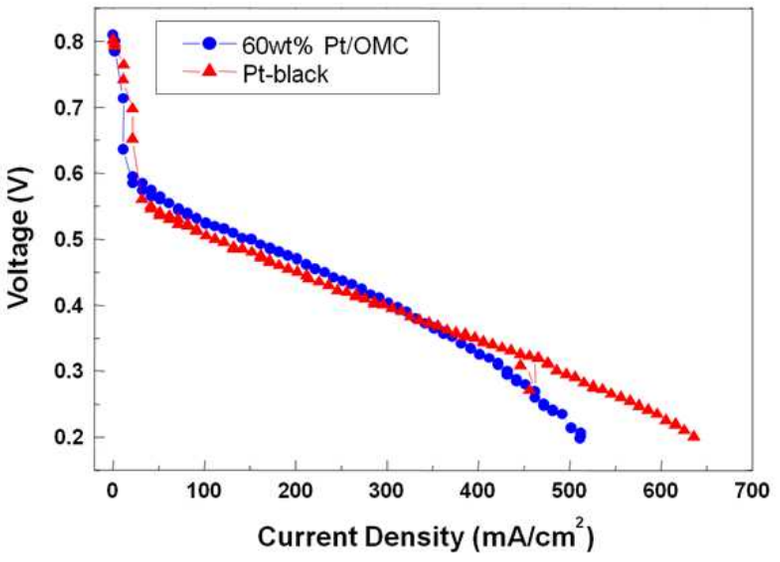

Figure 12. Comparison of polarization curves at 70 ◦C of MEA with the cathode from Pt/OMC catalyst (2 mg/cm^2) and unsupported Pt black catalyst (6mg/cm^2) (cathode feed: air, anode feed: 1M CH_3OH).

5. Conclusion

In this chapter, the fabrication processes for the electrode for MEA was briefly reviewed in a view of optimization of process parameter and application of new supported catalyst. The processes were catalyst coated on the electrode (CCE), decal transfer catalyst coated on membrane (DTM) and direct catalyst coated on membrane (DCM) methods. Among the three processes, the optimization of DCM method for DMFC MEA was presented as an example. The temperature and pressure were the main parameter which should be adjusted for maximizing the performance of MEA using hydrocarbon membrane. The effect of pore generation by pore forming agent on the performance was discussed. In addition, the application of new Pt/OMC catalyst for DMFC MEA was demonstrated by controlling the amount of ionomer and compression of catalyst layer. The application of Pt/OMC catalyst resulted in the decrease of the amount of Pt in the cathode from 6 mg/cm^2 for Pt black catalyst to 2 mg/cm^2 using Pt/OMC without lost the performance.

Author details

Chanho Pak, Dae Jong You, Kyoung Hwan Choi and Hyuk Chang
Energy Lab, Samsung Advanced Institute of Technology, Samsung Electronics, Co. Ltd., Republic of Korea

6. References

Andujar, JM. (2009). Fuel Cells : History and updating. A walk along two centuries. *Renewable and Sustainable Energy Reviews*, Vol.13, No.9, (December 2009), pp. 2309-2322, ISSN 1364-0321

Chang, H. (2007). Synthesis and characterization of mesoporous carbon for fuel cell applications. *Journal of Materials Chemistry*, Vol.17, No.30 (May 2007), pp.3078-3088, ISSN 1364-5501

Cho, J. (2009). Fabrication and evaluation of membrane electrode assemblies by low-temperature decal methods for direct methanol fuel cell. *Journal of Power Sources*, Vol.187, No.2, (February 2009), pp. 378–386, ISSN 0378-7753

Frey, Th. (2004). Effects of membrane electrode assembly preparation on the polymer electrolyte membrane fuel cell performance. *Electrochimica Acta*, Vol.50, No.11, (November 2004), pp. 99-105, ISSN 0013-4686

Guan, R. (2006). Effect of casting solvent on the morphlogy and performance of sulfonated polyethersulfone membranes. *Journal of Membrane Science*, Vol.277, No.29, (June 2006), pp.148-156, ISSN 0376-7388

He, W. (2010). Oxygen reduction on Pd_3Pt_1 bimetallic nanoparticles highly loaded on different carbon supports. *Applied Catalysis B: Environmental*, Vol.97, No.18, (April 2010), pp.347-353, ISSN 0926-3373

IEA (Interational Energy Agency) (2010). Energy Technology Perspectives from http://www.iea.org/papers/2009/ETP_2010_flyer.pdf

Joo, S. (2001). Ordered nanoporous array of carbon supporting high dispersions of platinum nanoparticles. *Nature,* Vol.412, No. 6843 (July 2001), pp.169-172, ISSN 0028-0836

Joo, S. (2006). Ordered mesoporous carbon (OMC) as supports of electrocatalysts for direct methanol fuel cells (DMFC) : Effect of carbon precursors of OMC on DMFC performances. *Electrochimica Acta,* Vol.52, No.15, (May 2006), pp.1618-1626, ISSN 0013-46868

Joo, S. (2009). Preparation of high loading Pt nanoparticles on ordered mesoporous carbon with a controlled Pt size and its effect on oxygen reduction and methanol oxidation reactions. *Electrochimica Acta,* Vol.54, No.14, (May 2009), pp.5746-5753, ISSN 0013-46868

Jun, S. (2000). Synthesis of New, Nanoporous Carbon with Hexagonally Ordered Meso structure. *Journal of American Chemical Society*, Vol.122. No.43 (November 2000), pp. 10712-10713, ISSN 1520-5126

Kim., H. (2008). Cathode catalyst layer using supported Pt catalyst on ordered mesoporous carbon for direct methanol fuel cell. *Journal of Power Sources,* Vol.180, No.2 (March 2008), pp. 724-732, ISSN 0378-7753

Kuver, A. (1994). Distinct performance evaluation of a direct methanol SPE fuel cell. A new method using a dynamic hydrogen reference electrode. *Journal of Power Sources,* Vol.52, No. 1 (November 1994), pp.77-80, ISSN 0378-7753

Lee., H. (2009). Ultrastable Pt nanoparticles supported on sulphur-containing ordered mesoporous carbon via strong metal-support interaction. *Journal of Materials Chemistry,* Vol.19, No. 33 (July 2009), pp.5934-5939, ISSN 1364-5501

Liang, ZX. (2004). FT-IR study of the microstructure of Nafion® membrane. *Journal of Membrane Science,* Vol.233, No.1-2 (April 2004), pp.39-44, ISSN 0376-7388

Lindermeir, A. (2004). On the question of MEA preparation for DMFCs. *Journal of Power Sources,* Vol.129, No. 2 (April 2004), pp. 180–187, ISSN 0378-7753

Liu, F. (2006). Optimization of cathode catalyst layer for direct methanol fuel cells: Part I. Experimental investigation. *Electrochimica Acta,* Vol.52, No.10, (September 2006), pp.1417-1425, ISSN 0013-46868

Liu, FQ. (2006). Low crossover of methanol and water through thin membranes in direct methanol fuel cells. *Journal of Electrochemical Society,* Vol.153, No.3, (January 2006), pp.A543–A553, ISSN 0013-4651

Mao, Q. (2007). Comparative studies of configuration and preparation methods for direct methanol fuel cell electrodes. *Electrochimica Acta,* Vol.52, No.10, (August 2007), pp.6763-6770, ISSN 0013-4686

Pak, C. (2009). Mesoporous Carbon-Supported Catalysts for Direct Methnaol Fuel Cells. *Electrocatalysis of Direct Methanol Fuel Cells,* (October 2009) pp.355-378. ISBN 978-3-527-32377-7

Pak, C. (2010). Nanomaterials and structures for the fourth innovation of polymer electrolyte fuel cell. *Journal of Materials Research,* Vol.25, No.11 (November 2010) pp.2063–2071, ISSN 0884-2914

Park, H-S. (2008). Modified Decal Method and Its Related Study of Microporous Layer in PEM Fuel Cells. *Journal of Electrochemical Society,* Vol.155, No. 5 (May 2008), pp.B455–B460, ISSN0013-4651

Park, I. (2010). Fabrication of catalyst-coated membrane-electrode assemblies by doctor blade method and their performance in fuel cells. *Journal of Power Sources,* Vol.195, No.7, (May 2010), pp. 7078–7082, ISSN0378-7753

Park, J. (2008). Mass balance research for high electrochemical performance direct methanol fuel cells with reduced methanol crossover at various operating conditions. *Journal of Power Sources,* Vol.178, No.1, (March 2008), pp.181-187, ISSN0378-7753

Perry, ML. (2002). A Historical perspective of fuel cell technology in the 20th Century. *Journal of Electrochemical Society*, Vol.149, No. 7, (July 2002), pp.S59-S67, ISSN0013-4651

Ramasamy, RP. (2009). Fuel cell – proton-exchange membrane fuel cells : Membrane-ElectrodeAssemblies, *Encyclopedia of Electrochemical Power source,* (November 2009), pp. 787-805, ISBN 978-0-444-52745-5

Robertson, GP. (2003). Casting solvent interactions with sulfonated poly (ether ether ketone) during proton exchange membrane fabrication. *Journal of Membrane Science,* Vol.219, No.1-2, (July 2003), pp.113-121, ISSN 0376-7388

Song, SQ. (2005). Direct methanol fuel cells: The effect of electrode fabrication procedure on MEAs structural properties and cell performance. *Journal of Power Sources,* Vol.145, No.2, (August 2005), pp.495-501, ISSN 0378-7753

Song, Y. (2005). Improvement in high temperature proton exchange membrane fuel cells cathode performance with ammonium carbonate. *Journal of Power Sources,* Vol.141, No.2 (March 2005), pp. 250-257, ISSN 0378-7753

Sun, L. (2010). Fabrication and evolution of catalyst-coated membranes by direct spray deposition of catalyst ink onto Nafion membrane at high temperature. *International Journal of Hydrogen Energy*, Vol.35, No.10, (June 2010), pp.2921-2925, ISSN 0360-3199

Tang, H. (2007). Performance of direct methanol fuel cells prepared by hot-pressed MEA and catalyst-coated membrane (CCM). *Electrochimica Acta,* Vol.52, No.11, (March 2007), pp.3714-3718, ISSN 0013-4686

Therdthianwong, A. (2007). Investigation of membrane electrode assembly (MEA) hot-pressing parameters for proton exchange membrane fuel cell. *Energy,* Vol.32, No.12, (December 2007), pp. 2401–2411, ISSN 0360-5442

Tucker, MC. (2005). The pore structure of direct methanol fuel cell electrodes. *Journal of Electrochemical Society,* Vol.152, No.9 (September 2005) pp.A1844–A1850, ISSN 0013-4651

Uchida, M. (1998). A Improved preparation process of very low platinum loading electrodes for polymer electrolyte fuel cells. *Journal of Electrochemical Society*, Vol.145, No.11, (November 1998), pp. 3708-3713, ISSN 0013-4651

Wei, Z. (2002). Influence of electrode structure on the performance of a direct methanol fuel cell. *Journal of Power Sources,* Vol.106, No.1-2 (April 2002), pp. 364-369, ISSN 0378-7753

Wilson, M. (1995). Low platinum loading electrodes for polymer electrolyte fuel cells fabricated using thermoplastic ionomers. *Electrochimica Acta,* Vol.40, No.3, (February 1995), pp. 355-363, ISSN 0013-4686

Xie, J. (2004). Ionomer Segregation in Composite MEAs and Its Effect on Polymer Electrolyte Fuel Cell Performance. *Journal of Electrochemical Society*, Vol.151, No.7, (June 2004) pp.A1084–A1093, ISSN 0013-4651

You, D. (2010). High performance membrane electrode assemblies by optimization of coating process and catalyst layer structure in direct methanol fuel cells. *International Journal of Hydrogen Energy*, Vol.36, No.12, (April 2011), pp.5096-5103, ISSN 0360-3199

Zhang, J. (2006). Effects of MEA preparation on the performance of a direct methanol fuel cell. *Journal of Power Sources*, Vol.160, No.2, (April 2006), pp.1035-1040, ISSN 0378-7753

Zhang, J. (2007). Effects of hot pressing conditions on the performances of MEAs for direct methanol fuel cells. *Journal of Power Sources*, Vol.165, No.1, (February 2007), pp73–81, ISSN 0378-7753